Sol–gel encapsulation for power electronics utilizing 3-Glycidyloxypropyltriethoxysilane and 3-Mercaptopropyltrimethoxysilane

Tobias Kohler[1,2] · Georg Hejtmann[1] · Stefan Henneck[1] · Martin Schubert[1] · Michael Guyenot[1]

Abstract

3-Glycidyloxypropyltriethoxysilane and 3-Mercaptosilane were used to prepare a composite together with aluminum oxide. The compound is a potential candidate for being used as inorganic encapsulation. FTIR results paired with head-space analysis revealed a hardening of the composite at above 130 °C and degradation of the sol–gel-network above 150 °C. The adhesion of these compounds was tested via shear tests. It showed, that the addition of 3-Mercaptopropyltriethoxysilane enhanced the adhesion on silver significantly. This is attributed to the covalent nature of the Ag-S bond, which is forming as compared to the solely dispersive forces, when 3-Mercaptopropyltriethxysilane is not used. By conducting the shear test under temperature activation energies for the breakages were calculated. These coincide well with the binding energy of Ag-S in case silver surfaces are examined. In the case of a copper surface, a mixture of covalent and dipole–dipole interactions are found, since the activation energy for breakage is smaller as the Cu-O bond energy.

Graphical abstract
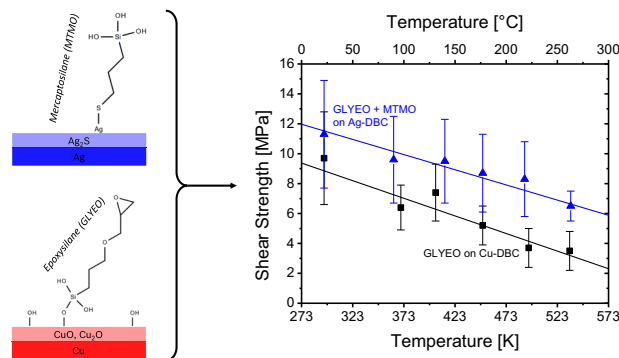
✉ Tobias Kohler
  tobias.kohler2@de.bosch.com

1 Robert Bosch GmbH, Renningen, Germany

2 Karlsruhe Institute for Technology, Karlsruhe, Germany

Springer

Highlights

- Novel encapsulation material using GLYEO and MTMO with Al_2O_3 fillers.
- Condensation reaction tracked with FTIR.
- Organic group of GLYEO degrades at elevated temperatures.
- High adhesion of composite at room temperature under thermal load.
- Adhesion mechanisms confirmed via shear strength evolution with temperature.

1 Introduction

The trend in power electronics points toward higher junction temperatures [1, 2], which highlights the need for investigating novel, stronger encapsulation materials. The encapsulation material covers the electronic device to protect it from humidity, spread the heat, and aims for fixation of the different parts so it is more robust against vibration and thermomechanical stresses. Thermomechanical stresses arise due to the different thermal expansion coefficients of the different materials and components inside the device. Usually, encapsulation of power electronics is done by either potting or molding. For this, silicones or epoxide resins are used. These exhibit high electrical resistance and high breakdown fields [3], which is crucial for encapsulation materials. However, they possess low thermal conductivities. To circumvent this, inorganic fillers are added to the encapsulation recipes. Down side is: they reduce the flowability even when spherical particles are used. Epoxy mold resins with filler contents around 80 wt% possess sufficient flowability only at elevated temperatures i.e., above 80 °C [4]. Even then, high pressures are needed to press them into a vacuum cavity with the electronics in. Silicones can be potted since they are well flowable. However, they do not bring sufficient mechanical stability to the system in order to stop the device from early failure due to thermomechanical stresses [5, 6]. In order to stabilize the device under thermomechanical loading, the encapsulation materials need to be stiff enough while adhering well to the substrate material as well as to the manifold components present in the device [6].

The encapsulation ideal case would be combining flowability with high strength, high thermal conductivity and excellent adhesion. Nowadays, this is not possible using polymeric matrix components like epoxies or silicones. Here always a trade-off between flowability and e.g., thermal conductivity is made. Both at the same time is not possible. For this reason, a new encapsulation class was introduced, the ceramic encapsulations. Käßner et al. [7] invented these under usage of cement-like systems with calcium-aluminate, ρ-alumina or magnesia as binder phases. These educts react with water resulting in the formation of hydroxides. As filler they were able to use Al_2O_3, which serves as a thermal conductivity booster. With this materialsystem, a well-flowable slurry can be produced for potting, which at the same time enables high thermal conductivity and high strength after hardening. Low viscosity results from using water in the mix, which is consumed during hardening. High thermal conductivity and high strength are gained due to the hardening by means of the hydraulic reaction of the reactive oxides embedding the highly thermal conductive aluminum oxide particles. However, several problems using these inorganic encapsulations were identified. Among them were corrosion of the metals, water uptake, limited potting time, and limited adhesion [8]. While corrosion of the metals and the water uptake could be reduced by measures concerning the recipe of the encapsulation, the potting time and the adhesion remain a bottleneck. Solely with workarounds like priming the surface of the electronics sufficient adhesion can be gained. However, this brings other difficulties like high CTE of the primer, which is seen as very critical [9].

In general, one needs a binder system that is well flowable, well-dispersing Al_2O_3, curing at temperatures above ambient, and forms a tough network when cured with good adhesion on metals. Thinking of these requirements a sol–gel-based system seems to be promising. It is well flowable in its monomer state and miscible with water, which is an excellent dispersion medium for Al_2O_3, forms a tough network when cured at elevated temperatures and adheres well to several metal surfaces. Additionally, it can provide enough thermal stability. Whilst the C-C backbones in organic polymers have bond stability of 618.3 kJ/mol [10], the Si-O bond-forming from the sol-gel process provides superior bond stability of 799.6 kJ/mol [10]. Due to that, a sol–gel composite is expected to be much more stable against temperature compared to organic polymers.

In this paper, a composite was developed exhibiting a binder phase consisting of an electrically insulating sol–gel system. While sol–gel systems (see Fig. 1) in general are well researched, the specific temperature window in which the electrical device will be operated has to be examined in more detail. Therefore, FTIR and headspace measurements were conducted for insights into the chemistry. One step further, the influence of temperature on the adhesion was tested. For this to do, the model systems of direct bonded copper substrates (Cu-DBC, exhibiting copper surface) and silver-covered direct bonded copper substrates (Ag-DBC, silver surface) were used (see Fig. 2).
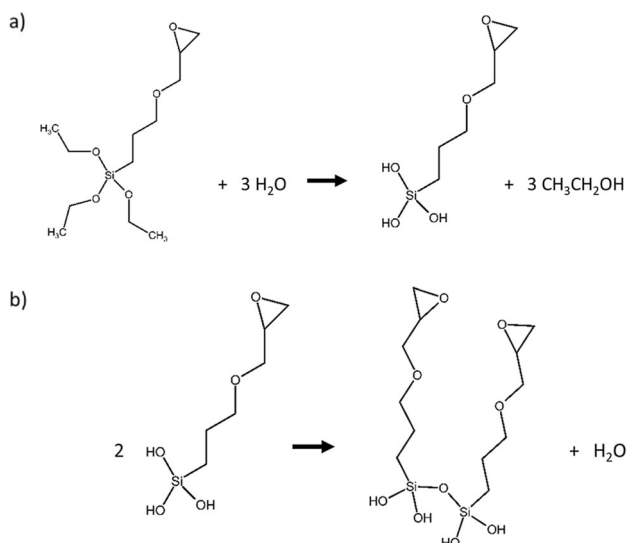
Fig. 1 **a** Hydrolysis reaction and **b** condensation reaction of GLYEO
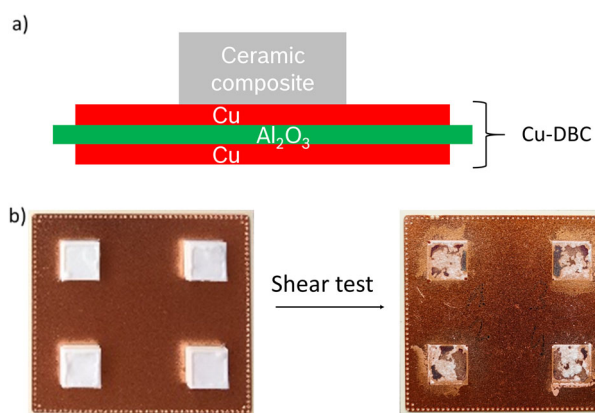
Fig. 2 **a** schematic setup of the Cu-DBC and the ceramic composite on top, **b** left real sample of ceramic composite on a Cu-DBC and right after shear test

2 Experimental

2.1 Sample production

Samples for FTIR and headspace measurements were made by mixing 3-Glycidyloxypropyltriethoxysilane (GLYEO) with water at a given ratio of 3:2. The mixture was vigorously stirred at 70 °C for 3 h. During that time the hydrolysis reaction according to Fig. 1a took place. Evidently, the smell of ethanol was recognized afterward. Optionally, 3-Mercaptopropyltrimethoxysilane (MTMO) was added to the hydrolyzed mixture. After the hydrolysis step, the condensation step according to Fig. 1b was performed in a furnace at >80 °C for 10 h. In fact, this step includes two events. First, the condensation reaction and second the evaporation of the water-ethanol solution, yielding a transparent sample with low mechanical strength and large

bubbles in it. These samples were taken to headspace analysis. Samples for FTIR were heat-treated before measuring the absorption spectra.

To gain high thermal conductivity, the samples for the shear tests, dilatometry, and scanning electron microscopy were prepared from the GLYEO/water mixture as described above with addition of Al_2O_3. Al_2O_3 was chosen since it possesses high thermal conductivity of about 30 W/(m·K), while at the same time having excellent electrically insulating properties [11]. The samples were treated at 80 °C for 10 h with a post-treatment at 150 °C for 10 h if no else was indicated. The samples appeared white with a slight yellowish surface.

With this, the process for sol–gel synthesis conducted here is dissimilar from most of the ones reported in the literature. Usually, organic solvents are added for hydrolysis to yield a single-phase liquid [12]. Here, no additional solvent apart from water was used, in order to minimize the amount of solvent to be evaporated later on. Secondly, neither acid nor base catalyst was used to perform hydrolysis. This is typically done to accelerate hydrolysis [12]. However, this brings additional contaminants to the mixture, which cannot be tolerated when applied to electronic modules. The risk of corrosion and dendrite formation increases drastically if such catalysts would be used.

3 Methods

For a detailed understanding of the network formation as well as for determining the chemical stability FTIR spectra were conducted. To do so, a Bruker Lumos 156 FTIR system in ATR configuration was used. It was measured from $600 \, cm^{-1}$ until $4000 \, cm^{-1}$. For further insights into the temperature stability, headspace analysis was used to determine the chemical deterioration products followed from thermal treatment. The measurement was performed using an Agilent 5975 mass spectrometer. The samples were held at the respective temperature for 2 h before analyzing the gas phase evolved during that time. The gas was analyzed by the aforementioned mass spectrometer. With scanning electron microscopy the microstructure of the samples was examined. The samples were prepared by conventional grinding with subsequent plasma milling. SEM analysis was performed using a Zeiss VP35 equipped with a field evaporation gun, a CCD camera, and an Oxford energy dispersive X-ray spectrometer. Dilatometry was used to determine the shrinkage of the sample body. Therefore, 2 cm long cylinders were prepared and measured with 2 °C/min up to 200 °C including a 20 h holding step at 200 °C. Additionally, the CTE of the sample was evaluated this way.

In order to analyze the adhesion, shear tests were performed using cuboid samples of $(5 \times 5 \times 2) \, mm^3$ in size as
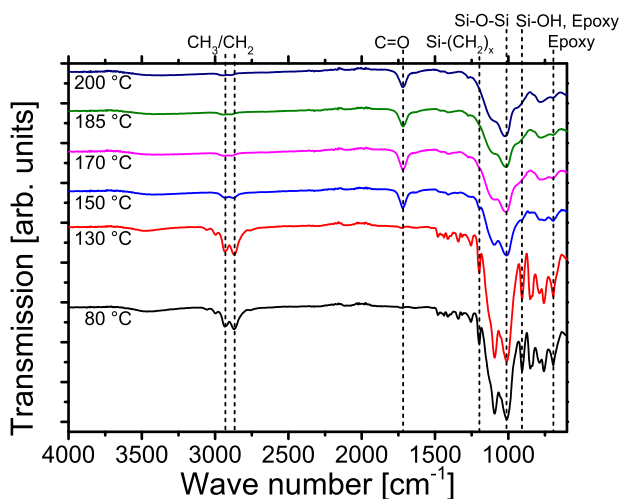
Fig. 3 FTIR spectra of a GLYEO/water mixture pretreated at 80 °C, 130 °C, 150 °C, 170 °C, 185 °C, and 200 °C

depicted in Fig. 2b. The samples were cast on direct bonded copper substrates (Cu-DBC) (see Fig. 2a) which possess a copper surface and silver-coated direct bonded copper (Ag-DBC) substrates, which possess a silver surface. Substrates were cleaned using 2-propanol prior to 25% citric acid solution, both in an ultrasonic bath. Samples were finished with 2-propanol again and dried with pressurized air. The substrates were cleaned directly before potting the sample to prevent formation of a thick oxide layer. To yield the cuboid shape of the sample on a substrate, a silicone mask was used which offers cavities to cast the slurry. The samples were demolded after the 80 °C step. Post-treatment was conducted at various temperatures. If not specifically indicated 150 °C was used for post-treatment.

4 Results and discussion

The samples of the GLYEO/water mixture were post-treated at 130, 150, 170, 185, and 200 °C. Also, a reference sample was not post-treated at all. Afterward, FTIR was conducted. The resulting spectra are shown in Fig. 3. As seen between 80 and 130 °C there is not much change in the spectra. The band structure is mostly identical to each other. Even though the reaction was reported to be exothermic, the activation barrier is quite high with 32.5 kcal/mol according to ref. [13]. Due to this, the energy barrier for reaction cannot be overcome and kinetics are very slow. As a result, with the sensitivity of this measurement procedure no change can be obtained. However, it cannot be excluded that there is minor change between 80 and 130 °C. Large difference is seen from 130 to 150 °C. However, increasing the temperature further, only minor changes progress until 200 °C. Marked changes are seen in the region between 600

and 950 cm^{-1}. The absorption bands almost completely vanish between 130 and 150 °C. Likewise the ones between 1200 and 1600 cm^{-1}. In contrast, a peak at 1720 cm^{-1} evolves during this temperature step. This peak can be assigned to the C=O bond [14]. Clearly, it develops due to the temperature rise. It might be present due to the oxidation of a secondary alcohol. Secondary alcohol is easily formed during ring opening of the epoxide, which will be looked at in more detail below.

Finally, the appearance of the peaks at 1000 to 1200 cm^{-1} changes (see Fig. 3). These peaks represent the Si-O-Si bonds with their stretching, bending, and out-of-plane movement. [15] While until 130 °C there are two distinct peaks seen, above 130 °C there is only one peak at lower wave numbers present with a shoulder on the high wave numbers side. The double structure at 130 °C might stem from both Si-O-Si and C-O-C excitements [16]. At above 130 °C the peak structure in this region resembles the spectra of a SiO$_2$ [15]. This leads to the suggestion that reactions take place that destroy or reorder the organic rest at the silicon atom. This hypothesis is also supported by the vanishing peaks below and above the 1000–1200 cm^{-1} region. Especially interesting are the epoxide excitements seen at 694, 906, and 1412 cm^{-1}, which vanish between 130 and 150 °C. These indicate that the epoxide ring is opened or even eliminated at above 130 °C. In case it is opened, the epoxide ring might also be able to contribute to the curing and crosslinking of the network. Furthermore, the Si-OH (at 906 cm^{-1}) can be seen until 130 °C. This is representative of the product after hydrolysis (compare Fig. 1). Interestingly this peak disappears together with the peaks of the organics. The Si-OH absorption vanishes due to the progressive reaction in the fashion of Fig. 1b, to form Si-O-Si bonds. Concluding this, the network formation is finished only when heating above 130 °C. This suggests that a post-treatment at 130 °C is not sufficient to drive the condensation reaction in reasonable time and reach high degrees of crosslinking. However, post-treatment at 150 °C is sufficient. With this, crosslinking is a thermally activated process. Furthermore, no major changes are seen above, showing that there is no need to go beyond 150 °C post-treatment. It is expected, that the post-treatment has an influence on the shear strength due to the different degrees of crosslinking, which will be discussed later.

In order to get more insights into the thermal behavior of the GLYEO/water mix, headspace measurements were conducted (see Fig. 4). Among, the strongest peaks no compounds were found that can be associated with silicon-containing species. This is crucial to clarify since evaporation of siliceous compounds is a well-known problem for silicones [17]. Silicones can deteriorate e.g., by back-biting or hydrolytic scission. By the former one, terminal Si-OH groups can attack the Si-O-Si backbone forming e.g.,
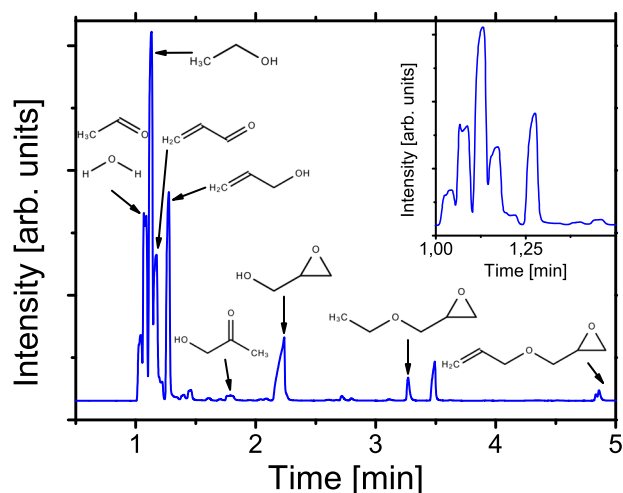
Fig. 4 Chromatography of the gases evolved during headspace analysis at 200 °C. In the graph, the most important molecules are assigned to the peaks and drawn

Fig. 5 SEM microstructure of the composite with the fillers and small gaps between filler and matrix components. The sample shown here was hardened at 150 °C

six-membered rings of alternating Si an O. Hydrolytic scission is basically the reverse reaction of the polycondensation. For more details about this reaction see the publication of Lewicki [18]. These cleavage products can reach the gas phase and condense on cooler parts or migrate along surfaces. Especially on optically or electrically critical parts, the outgassed molecules can degrade the performance of the system. [18] Thus, evaporation of siliceous compounds is alarming when designing an encapsulation material for high-temperature applications. It is believed, that the high degree of crosslinking of the compounds presented here prevents the emergence of siliceous deterioration products. For this reason, no contact loss is expected to be seen in electronic applications using these compounds.

During headspace analysis, ethanol was detected (see Fig. 4) most likely as a result of incomplete hydrolysis during the synthesis. During heating the heat forced the ethoxy-group to be cleaved from the silicon atom, resulting in ethanol outgassing. Furthermore, almost all of the compounds detected can directly be associated to the GLYEO. In more detail, the species seen in the mass spectrometry are parts ripped off the organic alkoxy-chain of the GLYEO. This indicates a deterioration of the organic part of the GLYEO by either temperature-induced pyrolysis action or by water-assisted hydrolytic scissoring. Since the headspace analysis was conducted in air, water for the hydrolytic reactions can stem from water uptake of the sample or from humidity in the air. This analysis showed that the organic part of the GLYEO is not very temperature stable. However, as far as this results not in drastic changes of the properties, the deterioration of the organic part is not regarded as severe for its application as encapsulation.

Since headspace analysis showed that there are evolving species during the post-treatment step, it is important to
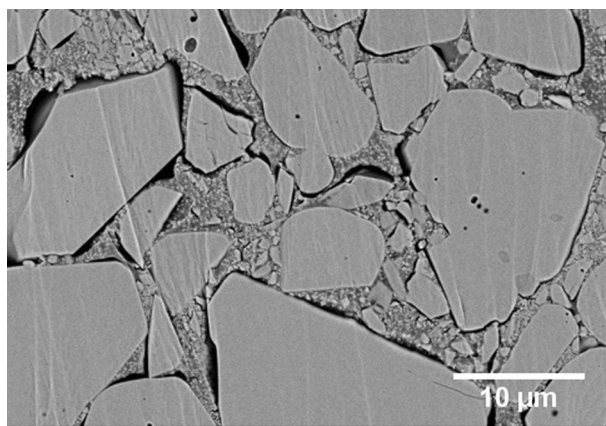
check the microstructure of the resulting compound. In the SEM picture seen in Fig. 5, the microstructure is shown of the compound, which includes the GLYEO/water mix and the Al_2O_3 fillers hardened at 150 °C for 10 h. The sol-gel matrix can be clearly distinguished from the fillers. Many filler particles are not well embedded in the matrix. Instead, small gaps between matrix and filler can be seen. This leads to a lower thermal conductivity and mechanical strength as it could be with well-embedded particles. The reasons for the gaps can be low adhesion of the binder phase to the particles or strong shrinkage of the material. First, one is very unlikely, since aluminum oxide possesses a thin layer of boehmite on its surface. The boehmite (AlO(OH)) should provide enough hydroxide groups to which the silanol can bind to. In Fig. 5, it can also be seen that there are still some connections left even of particles, which exhibit a wide gap between them and the filler. Thus, adhesion might not be the right explanation for the separation. The second option appears way more likely. During evaporation of the solvents pronounced shrinkage can be expected as well as during polycondensation due to the outgassing of water (compare Fig. 1). Since solely the matrix shrinks, stress can build up between the particles and the matrix leading to detaching, allowing the matrix to shrink further. However, also the evaporation itself may assist formation of gaps. When solvents built up an inner pressure to evaporate, this pressure can be released by opening a gap between particles and matrix where the gases can flow in. In addition, as seen in the headspace measurements, even at higher temperature, after the evaporation of the solvents, there are species found leaving the bulk. This further enhances the shrinkage of the binder phase and contributes to the inner pressure. By choosing another alkoxysilane having a more stable organic rest, this outgassing at higher temperatures could be avoided. Investigating this is a task for further research. However, the outgassing of water based on polycondensation

cannot be avoided due to the underlying reaction mechanism. If this is the cause for the detachment other solutions to the problem must be found.

Nevertheless, the samples appear to be hard and mechanically stable, but brittle due to their ceramic like nature. Furthermore, the thermal conductivity resides at about 6 W/(m·K), which is way higher than the commercially available encapsulation materials, even when they are filled with ceramic particles. Thus, it has to be clarified, if the gap formation due to shrinkage is a problem for the specific application as an encapsulation material.

In general, the shrinkage has to be kept as small as possible since this brings additional stress to the electronic material, which is especially relevant under temperature cycling conditions. Dilatometry was performed to check the shrinkage as well as the CTE of the compound. The samples were not post-treated before bringing it to the dilatometry, so it was only exposed to 80 °C. Two different recipes are shown. One containing a high amount of the sol-gel binder and one a rather low amount of sol–gel binder. It can clearly be seen that the shrinkage with a low binder content is way smaller. Even in a second and third run of the same sample irreversible shrinkage is seen, when using higher amounts of binder. The shrinkage might not be seen in the case of low binder content, since the filler particles touch each and hinder further shrinkage. This phenomenon also explains the detachment of the matrix from the fillers as seen in Fig. 5. In contrast, having a high binder content, filler particles are well separated and shrinkage of the binder is observed as seen in Fig. 6a.

The CTE was measured to be 6.9 ppm/K, which coincides well with the value for aluminum oxide [11]. The high filling of above 60 vol% (filler content) leads to low distances between the particles or they even touch each other as can be seen in Fig. 5. Due to this, the CTE follows the trend of aluminum oxide. Having a small CTE can be beneficial for encapsulation of an electronic module [19]. Very often the high CTE of the polymer encapsulations is one of the reasons why they reach their end of life, e.g., by bond lift-off. At 200 °C the samples were measured isothermal for 20 h. During this holding, a shrinkage with time of less than 0.02% for low binder content is observed. This is extremely small. Also, it can be seen from Fig. 6b, that the shrinkage takes place in the first 2 h after the start of the holding time. In contrast, for high binder contents larger shrinkage of more than 0.1%. On a time scale, the major shrinkage is until 10 h after reaching 200 °C. The reason for this is twofold. First, the binders polycondensation causes shrinkage thus the more binder is used, the more water has to be evaporated and the more shrinkage is expected. Second, fillers are well separated when using higher binder contents which results in unconstrained shrinkage of the binder.
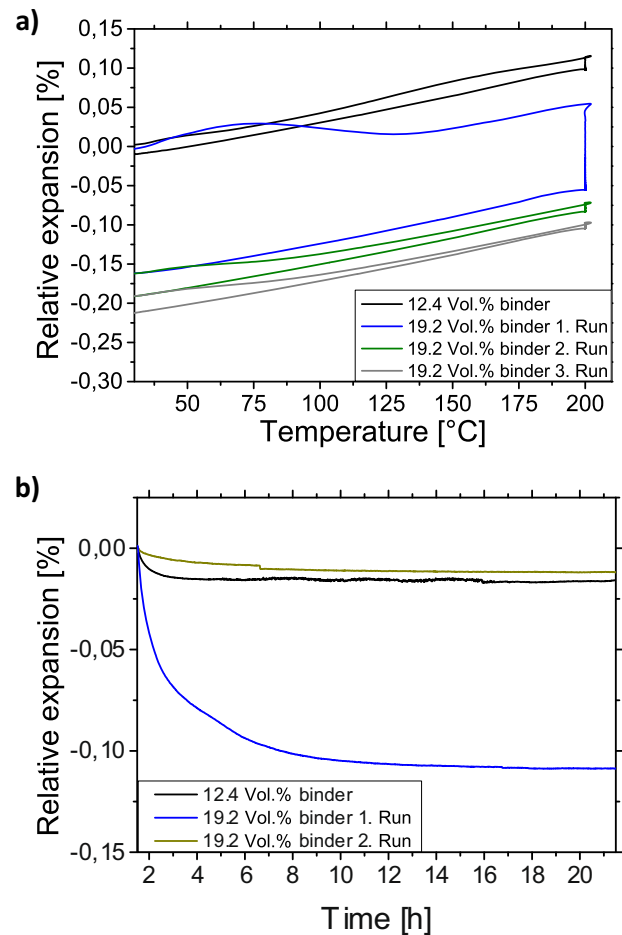
Fig. 6 **a** Length change as a function of temperature and **b** at 200 °C as a function of time measured by dilatometry. The binder contents are given in the graph

Taking an epoxy mold compound as a reference a thermal expansion of around 6–28 ppm [4] and shrinkage during molding of around 0.1% [20], is the benchmark. Also, epoxy compounds as being a polymer possess a glass transition temperature, which should not be crossed in application. Going above the glass transition temperature results in even higher CTE [4] and drastic lowering of the mechanical strength. As seen in the dilatometry, the compound introduced here exhibits no glass transition temperature instead, possessing low CTE over the whole range up to 200 °C. Due to this low CTE, it aims for fixation of the bond wires [19] and lower curing shrinkage resulting in less stress induced. Since the stresses under the cyclic load of temperature are one of the major reasons for failure of power electronic devices [19], these properties should provide the electronic part with increased lifetime compared to conventional polymeric encapsulation. As seen from the dilatometry the CTE is primarily dictated by the filler component. Thus, the CTE can be tailored to the CTE of the electronic part. For example adding fused silica (~0.5 ppm/

K [21]) as a filler the CTE is expected to decrease further. In contrast, if a larger CTE is required zirconia (~10.5 ppm/K [22]) for example could be utilized.

The property of having low shrinkage and low CTE will only have an effect, if at the same time the adhesion on the materials of the electronic module is good. Otherwise, the encapsulation will simply delaminate form the surface and have no effect like clamping the bond wire with its low CTE. Two important materials studied here, as a model system for the adhesion, are copper and silver. Copper is one of the most used metals on the surface of high-performance substrates like Cu-DBC substrates and AMB substrates. Thus, adhesion towards copper is very crucial. Silver emerges as getting more important in the future being the top surface of substrates for electronic modules. Hence, as a minimum requirement we define the adhesion of the encapsulant on copper and silver. The adhesion was tested using a shear test, being well aware that not exclusively the adhesion is tested, but also the intrinsic mechanical strength for the case that the adhesion is stronger than the mechanical strength of the compound.

Adhesion on copper is easily realized with the given sol-gel systems. The Si-OH groups can perform a condensation reaction with the native copper oxide and its hydroxide groups to yield a covalent linkage across the interface promising high shear strengths [23]. Additionally, the epoxy group of the GLYEO might contribute to the interfacial strength by the polar oxygen or even by ring opening a linking to the OH-surface groups. Also, the polar groups like OH, Si-OH, and C-O-C can contribute through dipole-dipole interactions to the resultant adhesion strength. High shear strengths of the compound on copper of above 10 MPa can be measured when doing a post-treatment at 150 °C. However, adhesion on silver is very low, having a shear strength of below 1 MPa. Silver usually reacts in air to form Ag_2S instead of an oxide [10]. Hence, there are no or at least not enough OH-groups available to bind to the silanol group of the sol-gel mix. The citric acid during the cleaning process of the substrates is supposed to remove the sulfide but still the shear values are bad. In a study by Yang et al. [24] the Ag_2S formation was observed to be quite slow, first adsorbing oxygen prior to Ag_2S formation. Thus, in the time scope between cleaning the surface and potting the samples the Ag_2S might not be reformed. However, the sol-gel mix cannot connect to a bare Ag surface. So both, Ag_2S and Ag, are not beneficial for the interfacial strength of the sol-gel mix. One opportunity to reach sufficient adhesion on silver though is a special treatment of the surface.

It was found that treating the cleaned Ag surface in boiling water for 90 min significantly enhances the adhesion as can be seen in Fig. 7. Ashkhotov et al. [25] examined an
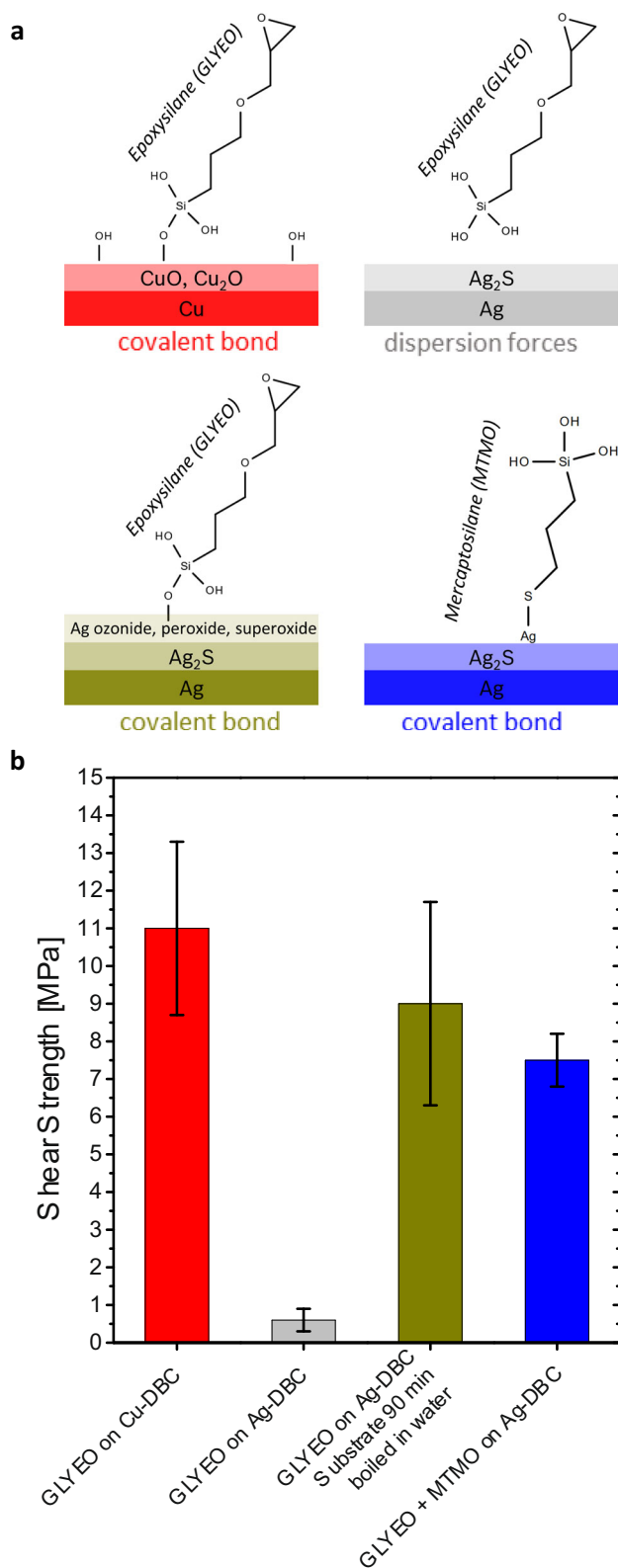
Fig. 7 a schematic picture of the covalent and dispersive bonding mechanisms with the substrates, **b** corresponding shear strengths of different processes and recipes on Ag-DBC and Cu-DBC. The respective bond mechanism is marked with the same color as the schematic substrate

Ag surface that was treated in 100 °C hot water vapor. It was found, that the oxidation introduces reactive oxygen species like peroxide, superoxide, or ozonide species at the Ag surface. These might be good ground for silanol linkage. Indeed the shear values reached are comparable to the ones yielded on copper suggesting a similar bond mechanism i.e., metal–O–Si linkages. Even though this works out well, from a process point of view, boiling substrates in water prior to encapsulation is critical. In a real case module, the electrical contact could be damaged during boiling it in water. Also, additional process steps are not wanted, since it costs money and time. Thus, a variant of the encapsulation material was developed which brings sufficient adhesion by its own. This was realized by using 3-Mercaptosilane in the sol–gel-mix. The thiol-group in this molecule is able to bind to the silver surface, due to the high affinity of silver towards sulfur. With that, the linkage is done not with the Si-OH group but the organic tail of the silanol molecule. Using this 3-Mercaptosilane again high shear strengths can be yielded on silver. From the two measures boiling the substrate and adding 3-Mercaptosilane in sol–gel-mix, the lather is the preferred one since it does not include an additional process step and is less critical for the electronic connections. However, further studies have to be conducted to check for potential corrosion effects using 3-Mercaptosilane.

As seen from the FTIR results the hardening temperature is expected to give influence the resulting shear strength. In Fig. 8a it can be seen, that the shear strength reaches its maximum, when treating the composite at 150 °C for hardening, which is true for the encapsulation material on the Cu-DBC and on the surface treated Ag-DBC. Lower temperatures are not sufficient to fully harden the composite and drive the reactions necessary for linking to the substrate, which is the condensation reaction. Higher temperatures degrade the adhesion between composite and substrate resulting in a slight decrease of the shear strength value. Drastic decrease is seen between 200 and 220 °C in the case of copper (see Fig. 8b). Two reasons for that may interplay. First, further degradation of the network and the substrate linkage proceeds. Second, copper oxidizes more rapidly at higher temperatures. This leads to Kirkendall voidening [26]. Thus accompanying to the copper oxidation voids are generated at the interface between the evolving copper oxide and the neat copper. These voids weaken this connection which leads to increased breakage of the oxide–metal interface [27]. This can be seen especially when analyzing the surfaces of the broken shear bodies. A clear increase of the copper content on the shear bodies bottom (where it was prior to shearing connected to the substrate) indicates this mechanism. The copper oxide still resides on the shear body since it broke off the neat copper. Consequently, the copper oxide/copper interface was weaker as compared to the interface copper oxide/ceramic encapsulation.
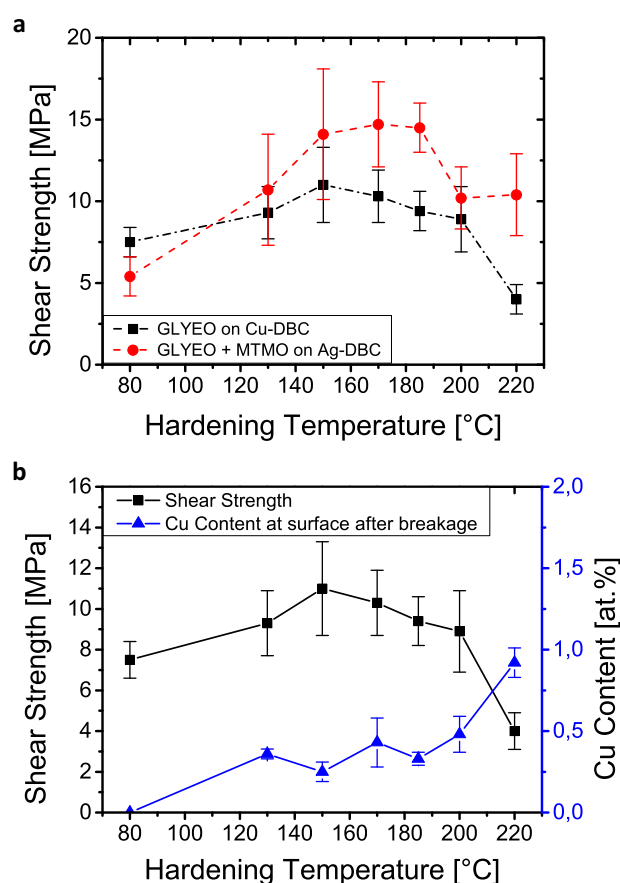

Fig. 8 a Shear strengths of the composites as a function of the hardening temperature, **b** shear strengths of the composite together with the Cu content on the breakage area, caused by rupture of the copper oxide layer at high temperatures

For the 3-Mercaptosilane modified encapsulation composite, the maximum is slightly shifted towards higher temperatures i.e., 170 °C with a more plateau-like behavior from 150 up to 185 °C. Furthermore, it is seen that the high-temperature adhesion at 220 °C is superior compared to the encapsulations without 3-Mercaptosilane. The 3-Mercaptosilane is able to bind to the Glycidyl-group of the GLYEO. This is a hardening mechanism in addition to the condensation reactions of the Si-OH groups. This leads to stronger network formation, being more temperature stable. However, the general trend of a dome-shaped progression of the shear strengths with temperature is the same for all the tested encapsulation composites.

In conjunction with the device, the encapsulation material has to attain adhesion under the influence of temperature. During operation, the semiconductor heats up due to its losses, same is for electrical connections. Thus, the adhesion on those materials must withstand the temperature influence of the device under operation. To test this, shear samples were heated on a heat plate and sheared in situ. This gives a realistic picture of the shear strength under
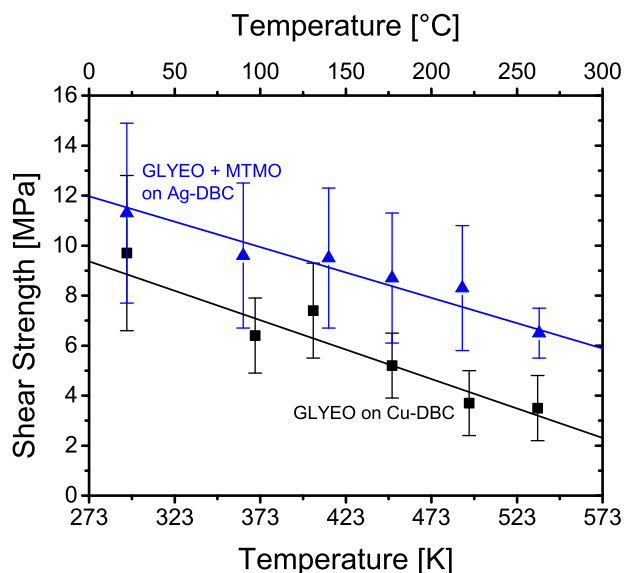
Fig. 9 Shear strengths measured while applying temperature as a function of temperature for the GLYEO variant on Cu-DBC and the MTMO variant on the Ag-DBC

Table 1 Showing several binding energies from [10] and [30] including the activation energies yielded from the fit of the shear values.

Bond	Binding energy [kJ/mol]
Literature Data taken from [10] and [30]	
Hydrogen bond (for H_2O, dipole-dipole interaction)	≈ 20
Ag–S (covalent bond)	216.7
Cu–O (covalent bond)	287.4
C–C (covalent bond)	618.3
Si–O (covalent bond)	799.6
Data of this work	
GLYEO-Composite on Cu-DBC	172 ± 53
MTMO-Composite on Ag-DBC	222 ± 41

thermal load. The results are depicted in Fig. 9. The shear values follow a linear decrease with temperature. From Vettegren et al. [28] this linear trend was already used for shear strengths to calculate an activation energy according to Eq. (1). They used several glues, including an epoxy resin. The glues showed, similar to the results here, a linear decrease of the adhesion with temperature. As shown by Anderson et al. [29] the process of degrading adhesion can be very intense for epoxy resins even when using an epoxy compound with a high glass transition temperature of above 250 °C. In this manner, it has to be regarded as success, that there is still above 3 MPa of shear strength at around 250 °C of the compound developed herein. Especially, the 3-Mercaptosilane modified one shows excellent adhesion at 260 °C of above 6 MPa.

$$\sigma = \frac{U_0}{\gamma} - \frac{k_B T}{\gamma} \cdot \ln\left(\frac{\tau}{\tau_0}\right) \tag{1}$$

where σ is the shear strength, γ is the interaction volume, τ is the time until breakage, T is the temperature, k_B the Boltzmann constant and U_0 is the activation energy. The activation energy was extracted from this equation by fitting it to the data (see Table 1). It can be seen, that the activation energy for breakage is larger for the 3-Mercaptosilane modified encapsulation on Ag-DBC as compared to the non-modified one on Cu-DBC. When comparing this to common binding energies, one immediately recognizes how close the activation energy lies to the covalent binding energies. In fact, for the compound with MTMO the activation energy is very close to the activation energy of the Ag-S bond. This suggests that the bonding mechanism

is shown above (compare Fig. 7) can be confirmed. However, the values in case of the copper surface are slightly smaller as compared to the covalent binding energies shown here, but larger as the dipole-dipole interaction energies (compare the hydrogen bond in a water arrangement). This implies that the binding mechanism is based on a mix of covalent bonds and dipole-dipole interactions. When taking the hydrogen bond of water and the Cu-O bond as a reference, the fraction of covalent interaction is around 57% against 43% dipole–dipole interaction. As already said the hydrolyzed GLYEO can condense with surface OH groups forming the covalent part of the bond mix. With the remaining OH-groups or with the polar oxygen atoms at the organic tail, the molecule can form hydrogen bonds, which are the dipole-dipole interactions in the bond mix. These binding mechanisms ensure very good adhesion even under thermal load.

5 Summary and conclusion

The novel compound developed here exhibits an opportunity to be used as an encapsulation material. It possesses high thermal conductivity, whilst having low CTE and good adhesion over a broad range of temperatures. The sol-gel process is the basis for this compound and enables these superior properties. The FTIR analysis matches the shear strength measurements, showing an optimal hardening temperature of 150 °C. The flexibility in the molecules that can be used for sol–gel is another advantage as seen for the silver surfaces. Easy adaption by introducing chemically suitable molecules in the mix can render desired properties of the compound. With that even on silver the crucial adhesion was successfully achieved. The mechanism of adhesion is a condensation to surface hydroxyl groups, yielding covalent bonding, in addition with dipole–dipole

interactions. The activation energy of adhesion degradation supports this suggestion. Especially, in the case of the silver surface, the difference between solely dispersive interactions (<1 MPa) and covalent linkages (>7 MPa) is shown. In case of copper, no purely covalent linkage could be reached, which was evaluated using the activation energy for breaking a bond. Here, a high degree of dipole–dipole interactions was found (43%). If for future works, the degree of covalent linkages can be enhanced, even higher shear values would be possible.

Compliance with ethical standards

Conflict of interest The authors declare no competing interests.

Publisher's note Springer Nature remains neutral with regard to jurisdictional claims in published maps and institutional affiliations.

References

1. Scheuermann U (2009) Reliability challenges of automotive power electronics. Microelectron Reliab 49(9–11):1319–1325. https://doi.org/10.1016/j.microel.2009.06.045

2. Txapartegi MG, Rosina M, Fuentes A (2018) Power module packaging 2018: material market and technology trends

3. Bartels O (2011) Leitfaden Anwendung und Verarbeitung von Vergussmassen für elektronische Baugruppen, Gesellschaft für Korrosionsschutz Arbeitskreis für Korrosionsschutz in der Elektronik und Mikrosystemtechnik. Frankfurt

4. Ardebili H, Zhang J, Pecht MG (2018) Encapsulation technologies for electronic applications. Elsevier, https://doi.org/10.1016/C2016-0-01829-6

5. Lutz J (2014) Packaging and reliability of power modules. CIPS 2014, In: 8th International Conference on Integrated Power Electronics Systems

6. Boettge B, Naumann F, Behrendt S, Scheibel MG, Kaessner S, Klengel S, Petzold M, Nickel KG, Hejtmann G, Miric AZ, Eisele R (2018) Material characterization of advanced cement-based encapsulation systems for efficient power electronics with increased power density. In: IEEE 68th Electronic Components and Technology Conference, https://doi.org/10.1109/ECTC.2018.00194

7. Kaessner S, Wichtner N, Hueller F, Berthold C, Nickel KG (2018) Novel cement-ceramic encapsulation material for electronic packaging. J Ceram Sci Technol 9(4):381–390. https://doi.org/10.4416/JCST2018-00024

8. Kaessner S, Scheibel MG, Behrendt S, Boettge B, Berthold C, Nickel KG (2018) Reliability of novel ceramic encapsulation materials for electronic packaging. J Microelectron Electron Packaging 15:132–139. https://doi.org/10.4071/imaps.661015

9. Kohler T, Hejtmann G, Rose K, Hirth E, Henneck S, Hoffmann MJ (2020) Ormocer-Primer for Improved Adhesion of Ceramic Composite Encapsulations. In: IEEE 26th International Workshop on Thermal Investigations of ICs and Systems (Therminic), https://doi.org/10.1109/THERMINIC49743.2020.9420490

10. Haynes WM (2010) Handbook of chemistry and physics. 91st Edition, CRC Press Inc

11. CeramTec (2021) The most well-known oxide ceramic material. CeramTec, Germany. https://www.ceramtec-industrial.com/en/materials/aluminum-oxide, Accessed 16 Dec 2021

12. Danks AE, Hall SR, Schnepp Z (2016) The evolution of 'sol-gel' chemistry as a technique for materials synthesis. Mater Horiz 3:91–112. https://doi.org/10.1039/c5mh00260e

13. Yang L, Feng J, Zhang W, Qu J (2010) Experimental and computational study on hydrolysis and condensation kinetics of γ-glycidoxypropyltrimethoxysilane (γ-GPS). Appl Surf Sci 257(3):990–996. https://doi.org/10.1016/j.apsusc.2010.07.102

14. Hernandez-Leon SG, Sarabia-Sainz JA, Montfort GRC, Huerta-Ocampo JA, Guzman-Partida AM, Robles-Burgueno MR, Burgara-Estrella AJ, Vazquez-Moreno L (2019) Bifunktional nickel-iminodiacetic acid-core-shell silica nanoparticles for the exclusion of high molecular weight proteins and purification of His-tagged recombinant proteins. RSC Adv 9:11038–11045

15. Shokri B, Abbasi-Firouzjah M, Hosseini SI (2009) FTIR analysis of silicon dioxide thin film deposited by Metal organic-based PECVD. In: 19th international symposium on Plasma Chemistry Society

16. Periathai RS, Rajagopal K (2014) FTIR and Raman vibrational investigations on the complex of pyridine with tartaric acid. IOSR J Appl Phys 6(4):09–12. https://doi.org/10.9790/4861-06430912

17. Lewicki JP, Liggat J, Pethrick R, Patel M, Rhoney I (2008) Investigating the ageing behavior of polysiloxane nanocomposites by degradative thermal analysis. Polym Degrad Stab 93:158–168. https://doi.org/10.1016/j.polymdegradstab.2007.10.008

18. Villahermosa RM, Ostrowski AD (2008) Chemical analysis of silicone outgassing. Proc SPIE 7069: Optical Syst Contam: Effects Meas Control 7069. https://doi.org/10.1117/12.802311

19. Wagner F, Maniar Y, Rittner M, Kaessner S, Guyenot M, Lang L, Wunderle B (2019) Simulative comparison of polymer and ceramic encapsulation on SiC-MOSFET power modules under thermomechanical load. In: 20th international conference on thermal, mechanical and multi-physics simulations and experiments in microelectronics and microsystems (EuroSimE), https://doi.org/10.1109/EuroSimE.2019.8724587

20. Hitachi (2021) Technical data sheet of Hitachi Chemical Epoxy molding compound, CEL-9220HF10, Hitachi, Malaysia. https://

e2e.ti.com/cfs-file/__key/communityserver-discussions-components-files/196/TDS-of-CEL_2D00_9220HF10.pdf. Accessed 22 Dec 2021

21. Souder W, Hidnert P (1926) Measurements on the thermal expansion of fused silica. Scientific papers of the bureau of standards 21(524)

22. Kyocera (2021) Technical Data Zirconia (Zirconium Oxide, ZrO_2). Kyocera, https://global.kyocera.com/prdct/fc/list/material/zirconia/zirconia.html. Accessed 22 Dec 2021

23. Arkles B (2014) Silane coupling agents: connecting across boundaries. 3rd edn., Gelest Inc, Morrisville

24. Yang X, Zhao Q, Han B, Zhao X (2008) Oxidation mechanism of silver thin films under room temperature and atmospheric environment. J Chin Ceram Soc 36(7):954–959

25. Ashkhotov OG, Khubezhov SA, Aleroev MA, Ashkhotova IB, Magkoev TT, Bliev AP, Kozirev EN (2018) Low-temperature oxidation of polycrystalline silver in water vapor. J Surf Investig: X-ray, Synchrotron Neutron Technol 12(3):513–515. https://doi.org/10.1134/S1027451018030059

26. Lee HJ, Yu J (2008) Study on the effects of copper oxide growth on the peel strength of copper/polyimide. J Electron Mater 37:1102–1110. https://doi.org/10.1007/s11664-007-0317-z

27. Cho SJ, Paik KW, Kim YG (1997) The effect of the oxidation of Cu-base leadframe on the interface adhesion between Cu metal and epoxy molding compound. IEEE Trans Compon, Packaging, Manuf Technol—Part B 20(2):167–175. https://doi.org/10.1109/96.575569

28. Vettegren V, Bashkarev AY, Sytov VA (2004) The temperature dependence of the strength of adhesion between epoxy-rubber glues and steels. Tech Phys Lett 30(2):99–101. https://doi.org/10.1134/1.1666952

29. Anderson BJ (2011) Thermal stability of high-temperature epoxy adhesive by thermogravimetric and adhesive strength measurements. Polym Degrad Stab 96(10):1874–1881. https://doi.org/10.1016/j.polymdegradstab.2011.07.010

30. Holleman AF, Wiberg N (1976) Lehrbuch der Anorganischen Chemie, 81–90 edn., De Gruyter